Low-temperature baroplastic processing of graphene-based polymer composites by pressure-induced flow

To cite this article: Wei Tang *et al* 2014 *IOP Conf. Ser.: Mater. Sci. Eng.* **62** 012023

Low-temperature baroplastic processing of graphene-based polymer composites by pressure-induced flow

Wei Tang[1], Cheng-en He[1], Yuanzhen Wang[1], Yingkui Yang[1,2] and Chi Pong Tsui[2]

[1] MOE Key Laboratory for Green Preparation & Application of Functional Materials, Faculty of Material Science & Engineering, Hubei University, Wuhan 430062, China
[2] Department of Industrial & Systems Engineering, The Hong Kong Polytechnic University, Hung Hom, Kowloon, Hong Kong, China

E-mail: yingkuiyang@gmail.com (YKY); gary.c.p.tsui@polyu.edu.hk (CPT)

Abstract: Two-stage emulsion polymerization was employed to synthesize nanoparticles consisting of a low glass transition temperature core of poly(*n*-butyl acrylate) (PBA) and a glassy poly(methyl methylacrylate) (PMMA) shell. Incorporation of graphene oxide (GO) into the PBA-PMMA latex produced GO/PBA-PMMA composites after demulsification and graphene/PBA-PMMA composites after chemical reduction of GO. The as-prepared powdery materials were processed into thin films by compression molding at room temperature as the result of a pressure-induced mixing mechanism of microphase-separated baroplastics. The presence of oxygen-containing groups for GO sheets contributed to better dispersion and stronger interface with the matrix, thereby showing greater reinforcement efficiency toward polymers compared to graphene sheets. In addition, both Young's modulus and yield strength for all materials increased with applied pressure and processing time due to better flowability, processability and cohesion at higher pressure and longer time. Low-temperature processing under pressure is of significance for energy conservation, recyclability and environmental protection during plastic processing.

1. Introduction

With extremely high values of Young's modulus (1.1 TPa) and fracture strength (125 GPa), thermal conductivity (~5×10^3 Wm/K), electrical conductivity (~6×10^5 S/m) and specific surface area (2630 m^2/g),[1, 2] graphene has thus great potential for improving the mechanical, thermal, electrical, and gas barrier properties of polymeric materials.[3] Over the past decade, considerable progress has been made for graphene-filled polymer composites.[4, 5] For instance, Chung *et al.*[6] prepared graphene/polystyrene (PS) composites by solution blending and subsequent compression molding, and obtained a low percolation threshold (0.19 vol.%) and an enhancement in storage modulus by ~28% at 1.94 vol.% of graphene loading. Macosko *et al.* [7] fabricated graphene/polycarbonate (PC) composites *via* melt compounding and observed better performance in suppressing gas permeability and tensile modulus relative to pure PC. We have recently employed an *in-situ* polymerization technology to fabricate graphene/poly(methyl methylacrylate) (PMMA) composites, which showed great increases in storage modulus (+58.3%) and glass transition temperature (T_g, +19.2 ℃) as well as high electrical conductivity (13.37 S/m) at 2.08 vol.% loading.[8]

Graphene oxide (GO) traditionally serves as a precursor for graphene,[9] however, it is also considered as a chemically-functionalized graphene containing epoxy/hydroxyl groups on the basal

plane and carbonyl/carboxyl groups at the edge.[10] GO has been increasingly attracting attention for its own characteristics.[11, 12] GO/poly(vinyl alcohol) (PVA) composite films could be simply fabricated by vacuum filtration and possessed high Young's modulus (4.8 GPa) and tensile strength (~110 MPa) for the film containing 3 wt.% GO. 132% and 36% of increases in tensile and compressive strengths have been reported for GO/PVA hydrogels upon addition of 0.8 wt.% GO, respectively.[13] Also, GO can effectively improve the compatibility of immiscible polyamide and polyphenylene oxide blends.[14] Recently, Liang *et al.* [15] have prepared GO/styrene-butadiene rubber (SBR) composites by aqueous-phase mixing of GO colloid with SBR latex in the presence of a small amount of butadiene-styrene-vinyl pyridine latex. The mechanical properties of GO/SBR composite with 2.0 vol.% GO was found to be comparable with those of the SBR composite reinforced with 13.1 vol.% of carbon black.

Till now, graphene- and GO-based composites have been frequently reported using various polymers including nylon, polyolefin, polyester, and polyimide.[4] Although these thermoplastic composites have been successfully prepared by solution mixing, melt compounding and *in-situ* polymerization methods,[3] they generally require high processing temperatures to enable compression and extrusion molding into final products or the desired forms for property measurement. However, the hot-melt processing causes not only energy consumption when heating the materials to form a melt, but also thermal degradation of polymers and organic additives, resulting in poor plastics' performance. In 2003, Mayes *et al.* [16] reported a novel class of "baroplastic" block copolymers consisting of a high-T_g shell of PS and a low-T_g core of poly(*n*-butyl acrylate) (PBA) or poly(2-ethylhexyl acrylate) (PEHA). These baroplastics could exhibit melt-like flow and hence be processed by compression molding and extrusion at 20-50 ℃ under external pressure through an apparent semi-solid partial mixing mechanism.[17] Moreover, the baroplastics were easily shredded and remoulded for ten times without evident property degradation.

In the present work, core-shell PBA-PMMA nanoparticles were prepared by two-stage emulsion polymerization. To this polymer latex was added an aqueous GO colloid to produce GO/PBA-PMMA composites after demulsification and reduced graphene oxide (RGO)/PBA-PMMA composites after chemical reduction of GO, respectively. As expected, the obtained polymer composites with a characteristic of baroplastics could be compression-moulded under pressure at ambient temperature. Mechanical properties at different applied pressure and processing time were investigated for PBA-PMMA, GO/PBA-PMMA and RGO/PBA-PMMA composites.

2. Experimental Section

2.1. Materials

Methyl methacrylate (MMA, 99%) and *n*-butyl acrylate (BA, 99%) were purified by washing with aqueous solution of NaOH (5 wt.%) and drying with anhydrous calcium chloride. Water was distilled and deionized before use. Pristine graphite powder (>95%), sodium dodecyl sulfonate (SDS, 99%), hydrazine hydrate (N_2H_4, 50-60%), 1-dodecanethiol (98%), acetone (97%), potassium persulfate (KPS, 99%) and other chemicals were purchased from the Sinopharm Group Chemical Reagent Co., Ltd (Shanghai) and used without purification unless otherwise stated. GO was prepared from graphite using a modified Hummers method.[8, 11]

2.2. Synthesis of core-shell PBA-PMMA latex nanoparticles

Core-shell polymer nanoparticles were synthesized by two-stage emulsion polymerization according to the procedure in a literature with minor change.[17] In the first stage, a 250 mL glass flask charged with deionized water (60 mL), acetone (9 g) and SDS (0.9 g) was flushed with nitrogen for 20 min, and the resulting solution was heated to 65 ℃ under vigorous stirring. To the above solution was slowly added 9 g of BA over a period of *ca.* 30 min and stirred for another 1 h. A solution of KPS

(0.18 g) in water (10 mL) was then added to initiate polymerization of BA and the reaction lasted for over 5 h at 65 ℃. In the second stage, MMA (9 g) was pre-emulsified by adding water (60 mL), acetone (9 g) SDS (0.27 g), and chain transfer agent of 1-dodecanethiol (0.18 g) under vigorous stirring for over 1 h. The pre-emulsified MMA solution was then added dropwise, with a flow rate of 2-3 drops/second, to the PBA emulsion, and the reaction was allowed to proceed at 65 ℃ with constant stirring for an extra 12 h. The as-prepared copolymer emulsion was reserved for the fabrication of GO/PBA-PMMA and RGO/PBA-PMMA composites.

2.3. Preparation of GO/PBA-PMMA and RGO/PBA-PMMA composites

For the preparation of GO/PBA-PMMA composites, 81 mg of GO was ultrasonically dispersed into 300 mL of water to obtain a yellow-brown colloid. The stable suspension of GO was mixed with the PBA-PMMA latex for about 1 h with stirring, affording a GO/PBA-PMMA composite emulsion. The GO/PBA-PMMA emulsion was further treated by hydrazine hydrate for 25 min to obtain a RGO/PBA-PMMA emulsion. All as-prepared emulsions were demulsified by addition of an aqueous solution (5 wt.%) of aluminum sulfate. The obtained precipitates were purified by washing with a mixture of methanol/water (v/v, 50/50) for several cycles to remove emulsifier and demulsifier. Finally, the resulting powders were dried under vacuum at room temperature in the presence of phosphorus pentoxide, yielding GO/PBA-PMMA and RGO/PBA-PMMA composites as well as pure PBA-PMMA materials, respectively. The loading amount of GO and RGO were about 0.5 wt. % in the composites.

2.4. Room-temperature processing of baroplastic materials

Powders of GO/PBA-PMMA, RGO/PBA-PMMA, and PBA-PMMA were processed into films by compression molding at room temperature on a Minitype Thermo-compressor (Bl-6170-C, Dongguan Baolun Instrument Co., China). The processing was carried out under pressures of 10-60 MPa for 3-9 min. The resulting films were cut into rectangle samples for tensile tests.

2.5. Characterization

Particle size distribution of polymer latexes was determined at 25 ℃ by dynamic light scattering (DLS) experiments on a Malvern HPPS5001 laser particle-size analyzer. Tg was measured on a TA differential scanning calorimeter (DSC, Q2000) at 10 ℃/min under nitrogen. Transmission electron microscopy (TEM) analysis was performed on a Tecnai G220 electron microscope operated at 200 kV. Two composites were also cryo-microtomed at -80 ℃ to obtain thin films (~70 nm) for studying the dispersion state of GO and graphene sheets in the polymer matrix. Tensile tests were conducted on a universal testing machine (CMT-4104, SANS, China) at a crosshead speed of 5 mm/min. Five specimens were measured and averaged for each batch of material samples.

3. Results and Discussion

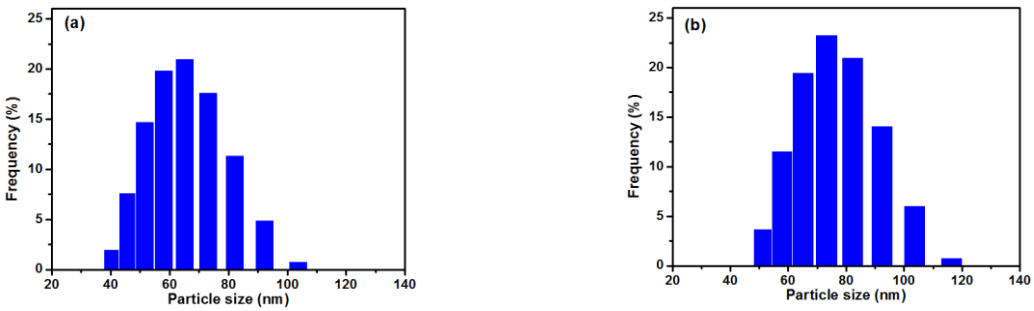

Figure 1. Particle size distribution histograms of (a) PBA core and (b) PBA-PMMA core-shell latex particles determined by DLS experiments.

Figure 1 gives particle size distribution histograms of the parent PBA core and PBA-PMMA core-shell particles. According to DSL data, the PBA core sizes obtained at the first stage of polymerization range from 35 nm to 110 nm in diameter (Fig. 1a), however, the PBA-PMMA core-shell particle sizes are in the range of 45-125 nm (Fig. 1b) after addition of MMA at the second stage. Their average particle sizes were calculated to be ~65 for core and ~76 nm for core-shell latexes, respectively. The increase of latex nanoparticles by ~11 nm in diameter implies an effective polymerization of MMA around PBA core. However, both PBA and PBA-PMMA latex particles show very large polydispersities due to the poor controllability of core and shell polymers during emulsion polymerization as described elsewhere.[17] TEM technique was further used to evaluate the particle sizes of PBA-PMMA latex. As shown in Figure 2, the average diameter of core-shell particles is approximately 75 nm, in good agreement with the DLS result (Fig. 1b).

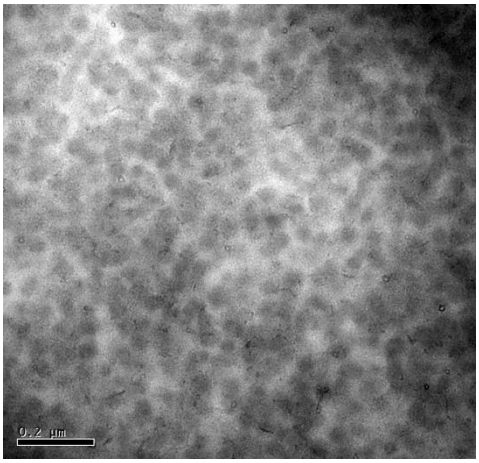

Figure 2. A typical TEM image of core-shell PBA-PMMA latex particles.

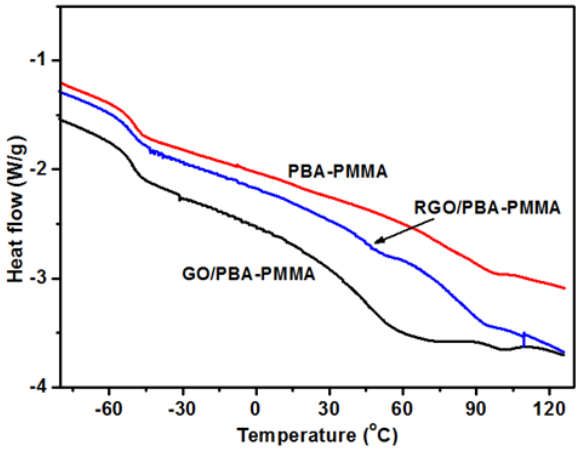

Figure 3. DSC curves of PBA-PMMA, GO/PBA-PMMA and RGO/PBA-PMMA composites.

Figure 3 shows DSC curves of GO/PBA-PMMA and RGO/PBA-PMMA composites and neat PBA-PMMA as dried. Two distinct T_gs for three samples occurs at about -45 ℃ and 105 ℃ corresponding to PBA core and PMMA shell, respectively, due to the microphase separation of PBA and PMMA components.[16, 17] Incorporation of GO and graphene into the matrix slightly increases T_gs of PBA-PMMA due to the mechanical interlocking and hydrogen bonding of crumpled sheets with polymer chains.[8] In addition, a new peak of T_g can be observed at around 55 ℃ for GO/PBA-PMMA and RGO/PBA-PMMA composites, which is properly ascribed to the interphase of two components.[17]

The PBA core is generally soft due to its intrinsically low T_g, however, the PBA-PMMA latex becomes a powdery product after demulsification due to the coverage of PBA surrounded by a high-T_g hard shell of PMMA, as shown in Figure 4. As reported previously,[16, 17] baroplastic nanoparticles consisting of a low-T_g soft core and a high-T_g hard shell can be processed by compression molding or extrusion at temperatures as low as room temperature. The white PBA-PMMA powders changed to the transparent films upon compression molding at a pressure of 35 MPa and room temperature (Fig. 4a), and the GO/PBA-PMMA composite changed from yellow powders to brown films after processing (Fig. 4b). However, the RGO/PBA-PMMA composite films appeared to be black-colored from grey powders due to the chemical reduction of GO (Fig. 4c). The low-temperature processing mechanism of PBA-PMMA and its composites results substantially from a pressure-induced miscibility between two-polymer phases, in which the applied pressure creates a mobile phase around portions of the glassy phase. Therefore, the low-T_g PBA layer acts as a “solvent” for the PMMA component. This enables flow of baroplastic materials and facilitates cohesion to the processed products.[16, 17]

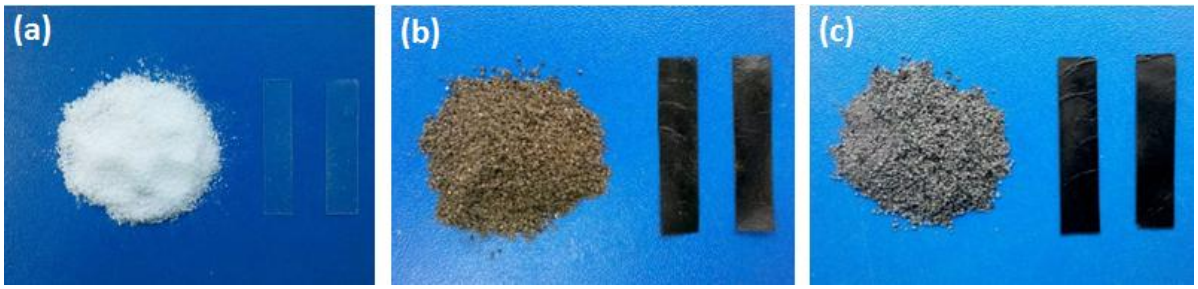

Figure 4. Original dried-powders of (a) neat PBA-PMMA, (b) GO/PBA-PMMA and (c) RGO/PBA-PMMA composites and their films processed by compression molding under 35 MPa for 5 min at room temperature.

Figure 5 shows TEM images of GO and graphene sheets dispersed in the composites processed by compression molding under 35 MPa for 5 min at room temperature. GO is readily dispersed in water or organic solvents because of polar groups,[18] while graphene sheets obtained by chemical reduction of GO tend to restack as a graphite-like structure.[19] Therefore, GO should show better dispersion than graphene in the latex and subsequent polymer matrix. As shown in Figure 5a, thin GO sheets with in-plane dimension (0.5~2 μm) are homogeneously dispersed in the matrix. In contrast, most of graphene sheets restack to form thick clusters in the matrix (Fig. 5b) due to the fact that the reduction of GO into graphene results in its hydrophobicity and re-agglomeration. It is noteworthy that these images imply that GO and graphene sheets might preferentially form segregated structures around the latex nanoparticles during mixing and precipitation, and the segregated sheets remain well after low-temperature compression molding. It is rationally accepted that these regions marked by white circles are supposed to be the latex particles before processing and the polymer phase after molding. Similar phenomena have been observed for Cu nanowire/PS [20] and graphene/PC [21] composites. Moreover, it should be noted that the core-shell nanostructure of PBA-PMMA could not be clearly discriminated in our TEM measurements because the PBA core or PMMA shell was not selectively stained by chemicals such as RuO_4 as described elsewhere.[17]

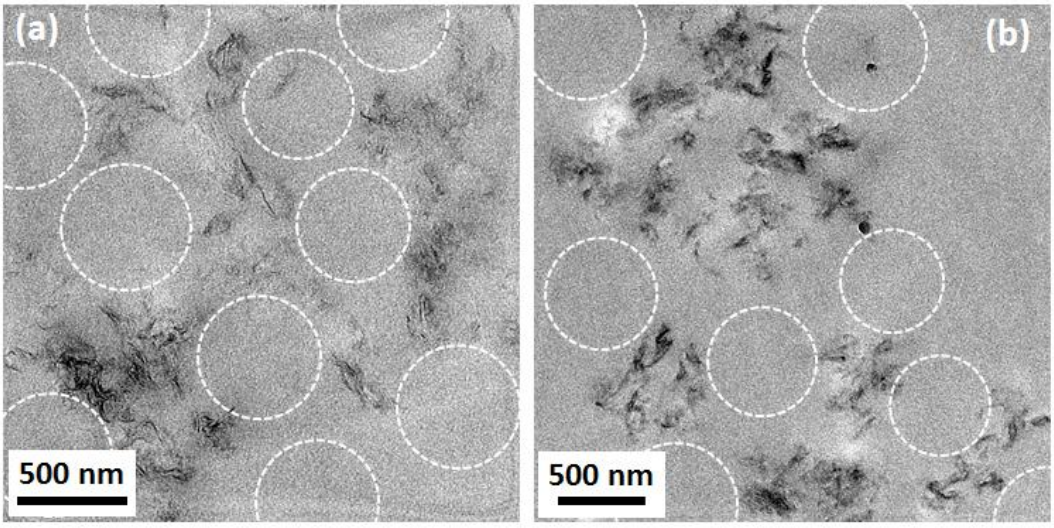

Figure 5. TEM images of (a) cryomicrotomed GO/PBA-PMMA, (b) RGO/PBA-PMMA composites, and white dash-circles correspond to the polymer phase coming from the core-shell latex nanoparticles.

Tensile tests were carried out on three kinds of baroplastic materials to examine their mechanical properties. Figure 6 shows the stress-strain curves for three materials processed by compression molding for 5 min with varied pressures (15-55 MPa) at room temperature. Tensile properties were found to be sensitive to the applied pressure, with Young's modulus and yield strength increasing with external pressure for each material. It can be also seen that both Young's moduli and yield strength of

all baroplastic composites gradually increase with processing time (from 3 min to 9 min) at a fixed pressure (35 MPa) and room temperature, as shown in Figure 7. The improved tensile properties are presumably due to better flowability, processability and cohesion of baroplastics induced by higher pressure and longer time.[17]

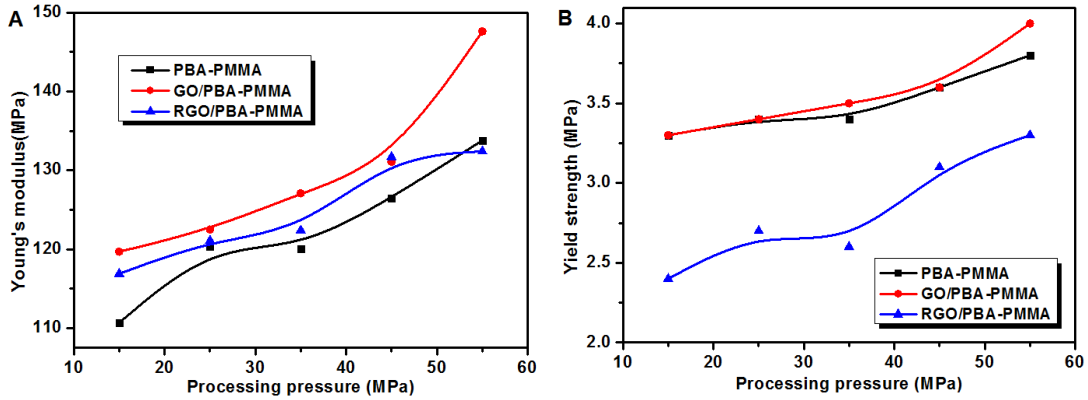

Figure 6. Young's modulus (A) and yield strength (B) of PBA-PMMA, GO/PBA-PMMA and RGO/PBA-PMMA composite films processed under different pressures for 5 min at room temperature.

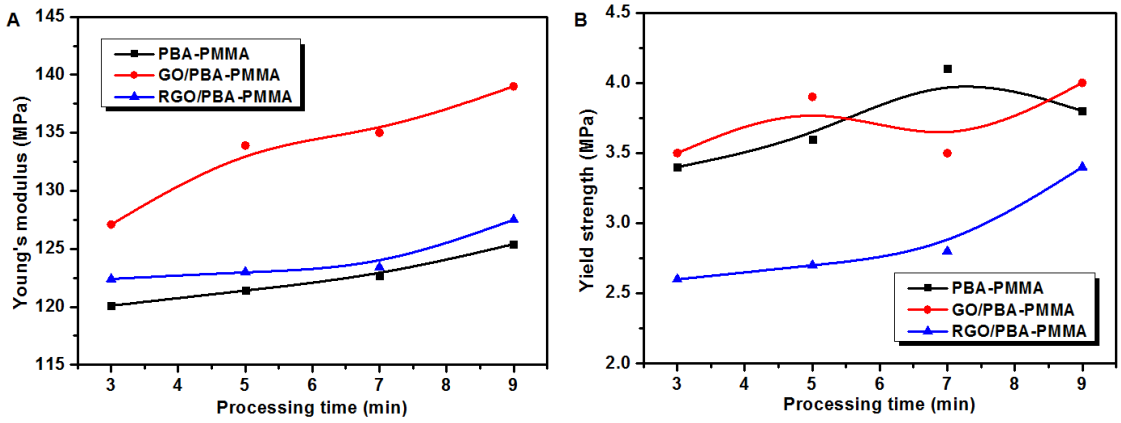

Figure 7. Young's modulus (A) and yield strength (B) of PBA-PMMA, GO/PBA-PMMA and RGO/PBA-PMMA composite films processed under 35 MPa at room temperature for different time.

Furthermore, incorporating graphene into the PBA-PMMA matrix slightly improves the composite's moduli but reduces yield strength because of the inefficient stress transfer and aggregated graphene sheets yielding high stress concentration sites in the polymer matrix.[22] However, both its modulus and strength are enhanced by adding the same loading of GO to PBA-PMMA. It is evident that the overall tensile properties of GO/PBA-PMMA composite show better improvements than RGO/PBA-PMMA relative to neat PBA-PMMA under identical processing conditions and comparable loading levels. This finding can be explained by three factors. First, GO shows better dispersion than graphene in the polymer matrix as shown in Figure 5. Second, oxygen-containing functional groups around GO can interact with pendant carbonyl groups of polymer chains *via* hydrogen bonding, forming a stronger interface with the matrix relative to graphene bearing less groups.[23] Third, GO is an insulator and not an optimum electrically-conductive filler for polymer composites, however, the moduli of GO sheets (208 GPa) [24] is very close to that of chemically-derived graphene (250 GPa).[25] This indicates a comparable efficacy of GO and reduced GO for the improvement of mechanical properties as previously reported in the PMMA composites.[26] Therefore, better dispersion and stronger interaction of GO relative to graphene in/with the polymer matrix achieve greater improvements in tensile properties for GO/PBA-PMMA composite.

4. Conclusions

Core-shell latex nanoparticles consisting of a PBA core and a PMMA shell were synthesized by a two-stage emulsion polymerization technique. Incorporation of GO aqueous solution into the PBA-PMMA latex successfully fabricated GO/PBA-PMMA and RGO/PBA-PMMA composites by *in-situ* reduction of GO. Coverage of a low-T_g soft core by a high-T_g hard shell resulted in powdery materials, which could be further processed into thin films by compression molding at room temperature due to the pressure-induced miscibility of microphase-separated baroplastics. GO showed better dispersion and stronger interaction in/with the matrix relative to graphene, thus achieving greater improvements in tensile properties for GO/PBA-PMMA composite. In addition, tensile properties for all materials were gradually improved with increasing external pressure and processing time because of better flowability, processability and cohesion between phases at higher pressure and longer time. The pressure-induced processing of baroplastic materials at low temperature reduces energy consumption, thermal degradation and processing time during plastic processing and also improves the recyclability.

Acknowledgments

We acknowledge the financial support from the National Natural Science Foundation of China (51073050, 51273057), the Program for New Century Excellent Talents in University (NCET-12-0709) and the Open Project of State Key Laboratory of Materials Processing and Die & Mould Technology (2012-P10) at Huazhong University of Science and Technology. CPT would like to thank for the support from Research Committee of The Hong Kong Polytechnic University (G-UB32).

References

[1] Allen M J, Tung V C and Kaner R B 2010 *Chem. Rev.* **110** 132
[2] Novoselov K S, Falko V I, Colombo L, Gellert P R, Schwab M G and Kim K 2012 *Nature* **490** 192
[3] Kim H, Abdala A A and Macosko C W 2010 *Macromolecules* **43** 6515
[4] Kuilla T, Bhadra S, Yao D, Kim N H, Bose S and Lee J H 2010 *Prog. Polym. Sci.* **35** 1350
[5] Peng RG, Wang YZ, Tang W, Yang YK and Xie XL 2013 *Polymers* **5** 847
[6] Pham V H, Cuong T V, Dang T T, Hur S H, Kong B-S, Kim E J, Shin E W and Chung J S 2011 *J. Mater. Chem.* **21** 11312
[7] Kim H and Macosko C W 2009 *Polymer* **50** 3797
[8] Yang YK, He CE, Peng RG, Baji A, Du XS, Huang YL, Xie XL and Mai Y-W 2012 *J. Mater. Chem.* **22** 5666
[9] Park S, Ruoff R S 2009 *Nat. Nanotechnol.* **4** 217
[10] Cai W, Piner R D, Stadermann F J, Park S, Shaibat M A, Ishii Y, Yang D, Velamakanni A, An S J, Stoller M *et al* 2008 *Science* **321** 1815
[11] Yang YK, He CE, He WJ, Yu LJ, Peng RG, Xie XL, Wang XB and Mai Y-W 2011 *J. Nanopart. Res.* **13** 5571
[12] Loh K P, Bao Q, Eda G and Chhowalla M 2010 *Nat. Chem.* **2** 1015
[13] Zhang L, Wang Z P, Xu C, Li Y, Gao J P, Wang W and Liu Y 2011 *J.Mater. Chem.* **21** 10399
[14] Cao Y W, Zhang J, Feng J C and Wu P Y 2011 *Acs Nano* **5** 5920
[15] Mao Y, Wen S, Chen Y, Zhang F, Panine P, Chan T W, Zhang L, Liang Y and Liu L 2013 *Sci. Rep.* **3** 2508
[16] Gonzalez-Leon J A, Acar M H, Ryu S-W, Ruzette A-V G and Mayes A M 2003 *Nature* **426** 424
[17] Gonzalez-Leon J A, Ryu S-W, Hewlett S A, Ibrahim S H and Mayes A M 2005 *Macromolecules* **38** 8036
[18] Paredes J I, Villar-Rodil S, Martinez-Alonso A and Tascon J M D 2008 *Langmuir* **24** 10560
[19] Stankovich S, Dikin D, Piner R, Kohlhaas K, Kleinhammes A, Jia Y, Wu Y, Nguyen S and Ruoff R 2007 *Carbon* **45** 1558
[20] Gelves G A, Al-Saleh M H and Sundararaj U 2011 *J. Mater. Chem.* **21** 829
[21] Yoonessi M and Gaier J R 2010 *Acs Nano* **4** 7211

[22] Yang YK, Yu LJ, Peng RG, Huang YL, He CE, Liu HY, Wang XB, Xie XL and Mai Y-W 2012 *Nanotechnology* **23** 225701

[23] Terrones M, Martin O, Gonzalez M, Pozuelo J, Serrano B, Cabanelas J C, Vega-Diaz S M and Baselga J 2011 *Adv. Mater.* **23** 5302

[24] Suk J W, Piner R D, An J and Ruoff R S 2010 *Acs Nano* **4** 6557

[25] Gomez-Navarro C, Burghard M and Kern K 2008 *Nano Lett.* **8** 2045

[26] Potts J R, Lee S H, Alam T M, An J, Stoller M D, Piner R D and Ruoff R S 2011 *Carbon* **49** 2615